

## N-induced soil acidification triggers metal stimulation of soil methane oxidation in a temperate steppe ecosystem

Lihua Zhang <sup>a,b,c,\*</sup>, Ivan A. Janssens <sup>d</sup>, Xinhao Zhu <sup>b,e</sup>, David Lipson <sup>e</sup>, Donatella Zona <sup>e</sup>, Fenghui Yuan <sup>b,f</sup>, Nannan Wang <sup>b</sup>, Yanyu Song <sup>b</sup>, Changchun Song <sup>b,\*\*\*</sup>, Yowhan Son <sup>g</sup>, Walter Oechel <sup>e</sup>, Xiaofeng Xu <sup>e,\*\*\*</sup>

<sup>a</sup> College of Life and Environmental Sciences, Minzu University of China, Beijing, 100081, China

<sup>b</sup> Northeast Institute of Geography and Agroecology, Chinese Academy of Sciences, Changchun, 130102, China

<sup>c</sup> State Key Laboratory of Vegetation and Environmental Change, Institute of Botany, Chinese Academy of Sciences, Beijing, 100093, China

<sup>d</sup> Department of Biology, University of Antwerp, Wilrijk, Belgium

<sup>e</sup> Biology Department, San Diego State University, San Diego, CA, 92182, USA

<sup>f</sup> Department of Soil, Water, and Climate, University of Minnesota, Saint Paul, MN, 55108, USA

<sup>g</sup> Division of Environmental Science and Ecological Engineering Korea University, Seoul, 02841, South Korea

### ARTICLE INFO

#### Keywords:

Nitrogen addition

pH

CH<sub>4</sub> oxidation

Metal element

### ABSTRACT

Methane (CH<sub>4</sub>) is a potent greenhouse gas, and it is well established that low nitrogen (N) stimulates- and high N suppresses CH<sub>4</sub> oxidation in grassland ecosystems. In this study, we examined the response of CH<sub>4</sub> uptake to long-term (>10 years) multi-level N additions in a temperate steppe of northern China. The N impacts on CH<sub>4</sub> uptake transitioned from positive to negative at the N addition rate of 4 g N m<sup>-2</sup> y<sup>-1</sup>. However, the high-N suppression on CH<sub>4</sub> uptake was partially relieved when the continuous (>10 years) high N inputs (16 g N m<sup>-2</sup> y<sup>-1</sup> to 64 g N m<sup>-2</sup> y<sup>-1</sup>) caused soil pH drop to < 5.7. Further experiments revealed that continuous high-N inputs acidified soil to pH < 5.7 that released metal ions to stimulate monooxygenase enzyme activity; therefore, the CH<sub>4</sub> oxidation suppression was partially relieved under continuous N loading. Structural equation model results confirmed that metal ions, such as Iron (Fe<sup>3+</sup>), Manganese (Mn<sup>4+</sup>), and Copper (Cu) desorbed by soil particles, were negatively correlated with soil pH while positively correlated with CH<sub>4</sub> oxidation under high N inputs. These analyses suggested that continuous high N inputs-induced soil acidification can release previously bounded metal elements that partially alleviated the N suppression on CH<sub>4</sub> uptake. The N-induced soil acidification impacts on CH<sub>4</sub> uptake might play a critical role in global CH<sub>4</sub> cycling and deserve further investigation as external N inputs continue climbing.

### 1. Introduction

Semiarid grasslands account for ~6% of the global sink of atmospheric methane (CH<sub>4</sub>), the second most potent greenhouse gas (Dalal et al., 2008; Dijkstra et al., 2013). External nitrogen (N) inputs have been reported to stimulate (Bodelier et al., 2000) or suppress (Tlustos et al., 1998) CH<sub>4</sub> uptake, depending on the rate and forms of the N added. Low N inputs typically stimulate the growth of methanotrophs that are always N-limited, thus enhancing the CH<sub>4</sub> oxidation in grasslands (King, 1992; Peng et al., 2019). On the contrary, high N inputs

typically suppress CH<sub>4</sub> oxidation via the competition between CH<sub>4</sub> and NH<sub>4</sub><sup>+</sup> molecules for CH<sub>4</sub> monooxygenases (Zhang et al., 2020), as confirmed by a continuous decline in CH<sub>4</sub> uptake under high N inputs in grasslands (Peng et al., 2019). Meanwhile, high N inputs acidify soils, thereby altering soil physical and chemical properties (Breemen et al., 1982; Horswill and Nauseef, 2008). Soil pH drop induced by continuous N might contribute to the suppression of CH<sub>4</sub> oxidation (Saarnio et al., 2004). However, the mechanisms of CH<sub>4</sub> oxidation suppression caused by N addition-induced soil pH drop remain elusive (Ambus and Robertson, 2006; Zhang et al., 2014).

\* Corresponding author. College of Life and Environmental Sciences, Minzu University of China, Beijing, 100081, China.

\*\* Corresponding author.

\*\*\* Corresponding author.

E-mail address: [zhanglihua@muc.edu.cn](mailto:zhanglihua@muc.edu.cn) (L. Zhang).

One possible mechanism is acidification caused-metal elements desorption from soil particles. For example, metal elements have been proven to affect  $\text{CH}_4$  oxidation due to their impacts on methanotrophs and methanogens, thus mediating  $\text{CH}_4$  flux (Stein, 2020). Iron (Fe), Manganese (Mn), and Copper (Cu) have direct and indirect impacts on microbial methanotrophy (Semrau et al., 2010; Semrau et al., 2013; Oni and Friedrich, 2019), and therefore  $\text{CH}_4$  uptake at the ecosystem level. The immediate impact is through the positive impacts of Fe and Mn on  $\text{CH}_4$  oxidation (Hakemian and Rosenzweig, 2007; Oni and Friedrich, 2019), likely due to their roles as alternative electron acceptors (Stein, 2020). The indirect effects occur by promoting enzyme activity (Krause et al., 2017). Through these direct and indirect impacts, soil microbes affect  $\text{CH}_4$  flux as regulated by metal elements (e.g., Cu) (Semrau et al., 2010, 2013). For example, the activity of Clade II nitrous oxide reductase (*NosZ*) is directly related to the  $\text{CH}_4$  cycling because some methanotrophs produce a copper chelator, named methanobactin, that has been shown to compete with  $\text{NH}_4^+$ , thereby increasing  $\text{CH}_4$  oxidation effectively (DiSpirito et al., 2016).

The soil consumption of  $\text{CH}_4$  is functionally intertwined with a range of other biogeochemically-active molecules, resulting in  $\text{CH}_4$  flux variations. Previous studies have suggested various mechanisms via which N affects soil  $\text{CH}_4$  uptake (Gulledge et al., 2004; Zhang et al., 2020), with an overall unimodal response to N additions (Bodelier and Laanbroek, 2004; Peng et al., 2019; Zhang et al., 2020). Although high-N inhibition on  $\text{CH}_4$  uptake over a short term has been widely accepted (Peng et al., 2019; Zhang et al., 2020), whether the suppression persists or there was a new transition along the N cumulative over time remains unknown. Integrating existing information to develop a holistic understanding of  $\text{CH}_4$  oxidation under N inputs is urgent to enhance our predictability of  $\text{CH}_4$  flux in terrestrial ecosystems under changing environments.

To address those gaps, we made use of a long-term field experiment (initialized in 2003) in which a semiarid grassland was exposed to a gradient of N applications (0, 1, 2, 4, 8, 16, 32, 64 g  $\text{N m}^{-2} \text{y}^{-1}$ ) to investigate the mechanisms of  $\text{CH}_4$  uptake under a gradient of N inputs over time. The primary objective was to explore the mechanisms via which N addition affects  $\text{CH}_4$  uptake along an N gradient. We hypothesized that (a) soil acidification caused by long-term N application (Tian et al., 2016; Malik et al., 2018; Xiao et al., 2020) enhanced the availability of metal elements such as Fe, Mn, Cu, and other soil ions (Ernani et al., 2002); and (b) higher metal availability stimulates methane monooxygenase (MMO) enzyme activity, thus partially relieving the N suppression on  $\text{CH}_4$  oxidation; this is built on the reported correlations between methane monooxygenase (MMO) enzyme activity and Cu (Hakemian and Rosenzweig, 2007), Fe, and Mn (Oni and Friedrich, 2019) concentration. The major implication is to clarify the role of soil acidification-related microbial methanotrophs acted in mitigating  $\text{CH}_4$  emissions to the atmosphere.

## 2. Materials and methods

### 2.1. Study site

This study was conducted in Duolun County ( $42^{\circ}02'N$ ,  $116^{\circ}70'E$ , 1324 m a.s.l.), a semiarid temperate steppe in Inner Mongolia, China. The mean annual precipitation and mean annual temperature are approximately 385 mm and  $2.1^{\circ}\text{C}$ , respectively. Low foothills characterize the topography at elevations of 1150–1800 m. The soil type is *Calcis-orthic Aridisol* according to the US Soil Taxonomy classification, with  $62.75 \pm 0.04\%$  sand,  $20.30 \pm 0.01\%$  silt, and  $16.95 \pm 0.01\%$  clay. The dominant plant species are *Stipa Krylov*, *Artemesia frigida*, *Potentilla acaulis*, *Cleistogenes squarrosa*, *Allium bidentata*, and *Agropyron cristatum*.

### 2.2. Experimental design

The N fertilization experiment was established in 2003. Seven N treatments (1, 2, 4, 8, 16, 32, and 64 g  $\text{N m}^{-2} \text{y}^{-1}$ ) and control (CK) with

eight replicates were randomly arranged in the areas of homogenous block to avoid heterogeneity within the plots, with  $10 \times 15$  m plots for each treatment. A 4 m wide buffer zone was set up to separate the adjacent blocks. The fields were annually fertilized by the urea, and the levels of N addition amounted to 0, 1, 2, 4, 8, 16, 32, and 64 g  $\text{N m}^{-2} \text{y}^{-1}$ , respectively, in the middle of July. Because the local fertilization time was in the growing season (May–September) and this study aimed to develop a mechanistic understanding rather than quantifying the annual budget, we did the measurements and observations in the growing season only.

### 2.3. Measurement of ecosystem $\text{CH}_4$ flux

We used a static chamber technique to measure the  $\text{CH}_4$  flux (Livesley et al., 2009) from 2013 to 2016. Briefly, three stainless steel permanent bases ( $50 \times 50 \times 12$  cm) with a 3-cm-deep groove for sealing water were inserted into soils down to 12 cm in the plots approximately a month before the measurement each year (Zhang et al., 2012). A stainless-steel top chamber (50 cm height) with heat-isolating and light-impenetrable material was installed outside the base, with the downside into the groove. The grooves were filled with water to seal the chamber. Two electric fans were installed on the inside top of the chamber to mix the air in the headspace continuously and thoroughly during the measurements (Zhang et al., 2014, 2020). Sixty-ml gas samples were collected at 10-min intervals for 30 min using sixty-ml syringes with airtight stopcocks. Simultaneously, the air temperature and pressure in the chamber were measured, and the soil temperature and moisture were measured at 5- to 10-cm depths using a thermometer (Spectrum Technologies, Inc. East - Plainfield, Illinois) and portable soil moisture measuring kit ML2x (ThetaKit, Delta-T Devices, Cambridge, UK), respectively. The  $\text{CH}_4$  concentrations of the gas samples were analyzed using a gas chromatograph (Agilent 7860, Agilent Technologies) equipped with a flame ionization detector (FID) using 60–80 mesh 13 XMS column (2 mm inner diameter and 2 m long), with an oven temperature of  $55^{\circ}\text{C}$ . Nitrogen with a flow speed of  $30 \text{ mL min}^{-1}$  was used as a carrier gas, and the  $\text{CH}_4$  flux was determined from the linear slope ( $r^2 \geq 0.95$ ) of the mixing ratio changes in four samples taken at 0, 10, 20, and 30 min after chamber closure. The  $\text{CH}_4$  fluxes were measured weekly from May to September in 2013, 2014, 2015, and 2016, and the positive fluxes indicated uptake.

### 2.4. Measurements of soil properties

Soil samples were taken to measure the soil total carbon (STC), total soil nitrogen (TN), total soil phosphorus (P), microbial biomass carbon (MBC), nitrogen (MBN), trace elements, and other physical properties (soil pH, texture, etc.). We took three soil cores to a depth of 10 cm from each plot once every month from May to September 2013–2016. The samples were mixed uniformly for each plot and separated into two sets. One set was stored at  $4^{\circ}\text{C}$  in the laboratory to determine MBC and MBN using the chloroform fumigation extraction method (Liu et al., 2014). The other was air-dried, sieved (2 mm), ground, and assessed for the determination of total C, N, P on a CNS elemental analyzer (Variomax CNS Analyser, Elementar GmbH, Hanau, Germany) and metal element (Fe, Mn, Cu, see the next section). Soil pH,  $\text{NH}_4^+$ , and  $\text{NO}_3^-$  were also measured in the laboratory. The soil samples stored at  $-20^{\circ}\text{C}$  were used for metagenomic analysis. The abundance of the *pmoA* gene was quantified by qPCR using primer pairs A189F/Mb601R (Cai et al., 2016). The PCR was performed in a 20- $\mu\text{l}$  mixture containing 10.0  $\mu\text{l}$  SYBR Premix Ex Taq (Takara), 0.5  $\mu\text{M}$  each primer, 2  $\mu\text{l}$  of DNA template, and ddH<sub>2</sub>O 7  $\mu\text{l}$ . All qPCR assays were performed on an ABI7500 Real-Time Detection System (Applied Biosystems, Inc., CA, USA). The relative abundance of methanotrophs was measured by Illumina Miseq, using primers A189F (5'-GGNGACTGGGACTTCTGG-3') and A601R (5'-CCGGMGCAACGTCYTTACC-3'). 644 genus microbial groups were detected and including three that participated in the  $\text{CH}_4$  oxidation

process (i.e., Methylosarcina, Methylocaldum, and Methylocystis).

## 2.5. Incubation experiments

To validate the metal impacts on  $\text{CH}_4$  oxidation, we designed an incubation experiment to quantify the impacts of Fe, Mn, and Cu on the  $\text{CH}_4$  oxidation rate with and without N addition. Meanwhile, we designed another incubation experiment to quantify the multi-N level impacts on  $\text{CH}_4$  oxidation rate, in which the  $\text{Fe}^{2+}$  and  $\text{Mn}^{2+}$  were measured, while  $\text{Fe}^{3+}$  was calculated as total Fe –  $\text{Fe}^{2+}$ , and  $\text{Mn}^{4+}$  was calculated as total Mn –  $\text{Mn}^{2+}$  (Lindsay and Norvell, 1978; Ferri et al., 2012; Wang and Hu, 2016) (the details are described in the section of 2.6). The soils for those incubation experiments were sampled from the adjacent sites that are 10 m away from the field experiment site. Four replicates of fresh soil, approximately 100 g each (moisture:10.1%), were sealed in 450 mL bottles. A total of 64 soils were filled with a plastic lid fitted with a rubber stopper and were incubated at 30 °C (the optimum temperature for  $\text{CH}_4$  oxidation) (Visvanathan et al., 1999). For the trace elements, 0.01 g N (applied as  $\text{NH}_4\text{NO}_3$ ), 0.286 g  $\text{Fe}_2\text{O}_3$  (0.2 g  $\text{Fe}^{3+}$ , 2 g/kg), 0.331 g  $\text{MnO}_2$  (0.2 g  $\text{Mn}^{4+}$ , 2 g/kg) and 0.2 g Cu (2 g/kg) (applied as copper powder), were added to each treatment, the amounts of added Fe, Mn, and Cu are based on the elemental variation concentration at the field site.

To ensure a sufficient mixture of the soil samples and metal, we put these reagents into 20 mL (water content kept at ~30% field capacity) deionized water (0.01 mol  $\text{L}^{-1}$   $\text{NH}_4\text{NO}_3$ ). All samples were incubated airtightly at 30 °C incubators. During incubation, we collected the gases in a wild-mouth bottle and measured  $\text{CH}_4$  concentration by meteorological chromatography (Ambient  $\text{CH}_4$  was used in these  $\text{CH}_4$  oxidation experiments) within 48 h.

The other 18 soil samples were incubated with 0, 0.01, 0.02, 0.05, 0.1, and 0.2 g N (0, 0.00179, 0.00357, 0.00893, 0.0179 and 0.0357 mol  $\text{L}^{-1}$   $\text{NH}_4\text{NO}_3$  solution with 20 mL, equals 0, 4.5, 9, 22.5, 45, 90 g N  $\text{m}^{-2}$  in field experiment state) with three replicates. Gas was extracted, and the  $\text{CH}_4$  concentration was measured by gas chromatography at the incubation time of 0, 3, 6, 12, 24, and 48 h. Then the  $\text{CH}_4$  oxidation rate was calculated with the fitted equation of  $y = ax + b$ ,  $y$  is the  $\text{CH}_4$  concentration, and  $x$  is the incubation time, the parameter  $a$  represents the  $\text{CH}_4$  oxidation rate (Fig. S8).

## 2.6. Metal measurements

The total Fe, Mn, and Cu were measured with the ICPS-500 (Shimadzu, Japan). Specifically, 0.5g air-dried soil samples were digested by  $\text{HNO}_3$ –HF– $\text{H}_2\text{O}_2$  (10:8:5). After digestion and complete deacidification, 20 mL  $\text{HNO}_3$  (1:4) and 10 mL HCl (1:1) were added to the solution and heated for 2 h. After filtering the sediments, the solution was diluted with deionized water to 50 mL. Finally, the ICP-500 was used to measure the metallic concentrations of the solution.

The  $\text{Fe}^{2+}$  and  $\text{Mn}^{2+}$  were measured by spectrophotometer (UV2550) (Beal et al., 2009; Amos et al., 2012). Specifically, 10.0000g fresh soil samples were put into a 250 mL conical flask, and 200 mL 0.1 mol  $\text{L}^{-1}$   $\text{Al}_2\text{SO}_4$  was added. After stirring thoroughly, the solution was diluted to 50 mL and added with 1 mL hydroxylamine hydrochloride. After being kept for a few minutes, 5 mL phenanthroline solution was drawn and used to measure the concentration of  $\text{Fe}^{2+}$  by using the spectrophotometer at the wavelength of 520 nm. Similarly,  $\text{Mn}^{2+}$  in soil was extracted by 0.1 mol  $\text{L}^{-1}$   $\text{Al}_2\text{SO}_4$ ,  $\text{Mn}^{2+}$  was oxidized to  $\text{MnO}_4^-$  by  $\text{KIO}_4$  in a neutral solution (pH = 7.0) and was measured by using the spectrophotometer at the wavelength of 525 nm.

The  $\text{NH}_4^+$ ,  $\text{NO}_3^-$ , TN, and TP were measured by a Flow analyzer (Seal AA3, Germany) (Yang et al., 2020). Specifically, 10 g sieved fresh soil samples were put into the centrifuge tubes, and 40 mL 2.0 mol  $\text{L}^{-1}$  KCl solution was added. After oscillation and centrifugation, the supernatant was extracted to measure the  $\text{NH}_4^+$ -nitrogen concentration. TN and TP were determined colorimetrically using a heating digestion method with

$\text{HClO}_4$ – $\text{H}_2\text{SO}_4$ . 0.5 g air-dried soil samples and 1g catalyzer mixed with  $\text{K}_2\text{SO}_4$  and  $\text{CuSO}_4$  (10:1) were put into digestion tubes and mixed with 5 mL  $\text{H}_2\text{SO}_4$  (Yang et al., 2020). After digestion, the solution was extracted to measure the concentration of N and P. The TC was measured using a Multi N/C 2100 TOC analyzer (Analytikjena, Germany) with a high temperature (1100 °C) combustion method. 0.1 g air-dried soil was placed into the combustion chamber and was kept for 1 h. We calculated soil TC as the weight loss as  $\text{CO}_2$ . After incubation, all the experimental and undisturbed soils were used for qPCR and sequencing analysis, following the same method described above.

## 2.7. Data analysis

Structural Equation Modelling (SEM) was performed to understand the N impacts on the  $\text{CH}_4$  oxidation and soil-microbe-metal interactions. Based on our knowledge of N impacts on  $\text{CH}_4$  oxidation, we developed a priori model, allowing a hypothesized causal interpretation of the linkages between soil acidification, microbe, metal elements, and  $\text{CH}_4$  oxidation. To test the hypothesis, we constructed conceptual models and determined the best fit with the SEM analysis. The hypothetical pathways of N impacts on  $\text{CH}_4$  oxidation were based on previous studies: (a)  $\text{CH}_4$  oxidation is primarily controlled by soil microbial and biochemical conditions (Hütsch, 2001), which is affected by N addition (Reischer et al., 2013); (b)  $\text{CH}_4$  oxidation is a biological process adjusted by N input-induced soil acidification (Tian et al., 2016). (c) Soil acidification induced by N addition triggers metal element desorption from soil particles, leading to the enrichment of metal elements that can alter  $\text{CH}_4$  oxidation (Hakeman and Rosenzweig, 2007; Oni and Friedrich, 2019). We used the abundances of the *pmoA* gene and  $\text{CH}_4$ -oxidizing bacteria as indicators for soil microbial activity (PC). The functional gene abundance represents the  $\text{CH}_4$  oxidation potential and its association with the  $\text{CH}_4$  oxidation rate at the ecosystem level in this study. Before running SEM, the N addition levels, pH, and  $\text{CH}_4$  oxidation were log-transformed to ensure normality. Analysis of variance (ANOVA) followed by Duncan's posthoc test was performed to test the N impacts on soil acidification, microbial activities, and metal elements. Differences were deemed to be significant if  $p < 0.05$ . Results from the best-fitting regression models were presented. SEM analyses were performed using the "lavaan" package in the R program (3.2 version).

## 3. Results

### 3.1. Nonlinear response of $\text{CH}_4$ uptake to long-term N addition

The field measurements showed that the semi-arid grassland functioned as a  $\text{CH}_4$  sink during the growing seasons (from May to September) of 2013 (10th year) - 2016 (13th year) (Fig. S1 a-d). The annual  $\text{CH}_4$  uptake ranged 1.40–4.47 kg  $\text{ha}^{-1} \text{y}^{-1}$ , with a strong inter-annual variability across the N gradient (Fig. S2). A humpback model that best characterized the relationship between  $\text{CH}_4$  response ratio (defined as  $\log(\text{CH}_4_{\text{treatment}}/\text{CH}_4_{\text{control}} * 100\%)$ ) and N addition rate in each of four measured years (Fig. 1a; Fig. S1 a-d), but the response ratio started to climb at the end of the treatment under the treatments of 16 g  $\text{m}^{-2} \text{y}^{-1}$  to 64 g  $\text{m}^{-2} \text{y}^{-1}$  (Fig. 1a), showing the alleviated-suppression from 10th to 13th year (Fig. 1b). The inhibition impact on  $\text{CH}_4$  uptake (expressed as  $\log(\text{CH}_4)$ ) decreased from 0.37 in the 10th year to 0.22 in the 11th year, 0.03 in the 12th year, and 0.025 in 13th year of N addition, suggesting the N-suppression on  $\text{CH}_4$  uptake was relieved from the 10th year to 13th year of N addition (Fig. 1b). At the level of 16 g  $\text{m}^{-2} \text{y}^{-1}$ ,  $\text{CH}_4$  uptake rates were 11.9% (2013), 18.2% (2014), 20.0% (2015) and 21.2% (2016) lower than those in control plots (Fig. S2 a-d). At the level of 32 g  $\text{m}^{-2} \text{y}^{-1}$ ,  $\text{CH}_4$  uptake rates were 37.3% (2013), 33.4% (2014), 20.8% (2015), and 21.7% (2016) lower than those in the control treatment (Fig. S2 a-d). Under the treatment of 64 g  $\text{N m}^{-2} \text{y}^{-1}$ ,  $\text{CH}_4$  uptake rates were 47.0% (2013), 39.4% (2014), 23.2% (2015), and 23.9% (2016) lower than the control treatment

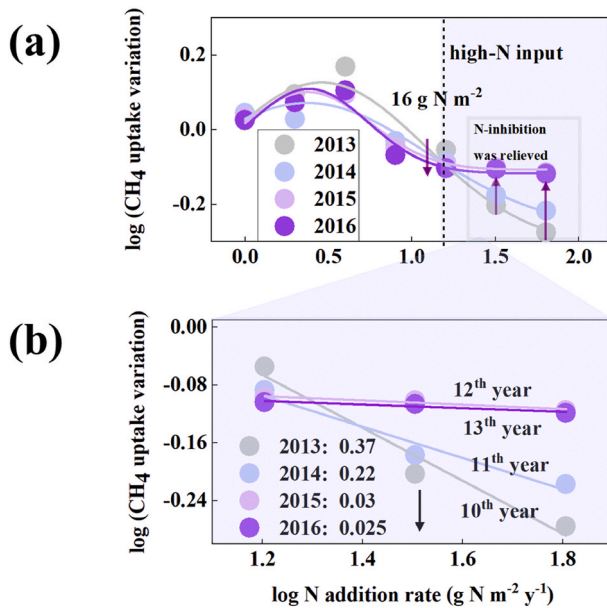


**Fig. 1.** N induced variation of  $\text{CH}_4$  oxidation in the grassland sites. Relationships between the N addition rate and the  $\text{CH}_4$  oxidation response ratio (the natural logarithm of the ratio between the treatment and control groups) over the four experimental years (2013–2016). The vertical line and light pink area indicate the second N threshold (from  $16 \text{ g N m}^{-2} \text{ y}^{-1}$ ) that alleviates the high N-suppression over time (a), and that was zoomed as (b); The Gaussian equation estimated the relationship:  $y = y_0 + a * \exp(-0.5 * (x - x_0) / b)^2$ , where  $y$  is  $\text{CH}_4$  oxidation response ratio,  $x$  is the natural logarithm of N application rate,  $y_0$ ,  $a$ ,  $b$ , and  $x_0$  are the fitted coefficients (a). The alleviation rate was shown as (b).

(Fig. S2 a-d).

We further explored the indirect impacts of N addition on  $\text{CH}_4$  uptake through its effects on soil properties and conditions. Across all N addition treatments, increases in soil  $\text{NH}_4^+$  (Fig. 2a) and  $\text{NO}_3^-$  (Fig. 2b) and

decreases in soil microbial biomass carbon (MBC, Fig. 2c) and soil pH (Fig. 2e) were observed. In contrast, soil microbial nitrogen (MBN) exhibited a humpback-shaped response curve with a maximum at  $8 \text{ g N m}^{-2} \text{ y}^{-1}$  N-addition (Fig. 2d). It was noted that soil pH decreased exponentially from 6.9 to 5.3, following:  $y = 4.95e^{5/(14.8+x)}$ , where  $x$  is the N addition rate,  $y$  is the pH value (Fig. S3 a). A significant difference was found between soil iron (Fe) content (Fig. S4 a) and manganese ion (Mn) (Fig. S4 b) in the field experiment, while small differences were found among the N treatments in soil copper (Cu) (Fig. S4 c). Strong stimulating impacts were found for Fe, Mn, Cu on  $\text{CH}_4$  uptake in the field experiment (Fig. 3a-c).

### 3.2. Impacts of elements (Fe, Mn, and Cu) on $\text{CH}_4$ oxidation

Results from the incubation experiment were consistent with those from the field experiments regarding metal impacts on  $\text{CH}_4$  oxidation. For instance, we found that Fe, Mn, and Cu stimulated the  $\text{CH}_4$  oxidation (Fig. 4a), promoted the abundances of *pmoA* (a genetic indicator for microbial oxidation strength (Boiesen et al., 1993; Ettwig et al., 2010)) (Fig. 4b) and  $\text{CH}_4$ -oxidizing bacteria (Fig. 4c). Specifically, increasing Fe, Mn, and Cu individually enhanced the  $\text{CH}_4$  oxidation rate by 85.2%, 85.6%, and 57.5%, respectively. At the same time, N addition ( $0.00893 \text{ mol L}^{-1}$  with 20 mL solution, equivalent to  $22.5 \text{ g N m}^{-2}$  in the field experiment) suppressed the  $\text{CH}_4$  oxidation rate by 79.3%. Concurrent applications of Fe and N, Mn, and N, or Cu and N enhanced the  $\text{CH}_4$  oxidation rate by 131.2%, 131.3%, and 142.2%, respectively (Fig. 4a). Adding Fe, Mn, and Cu alone increased the *pmoA* abundance by 44%, 43.4%, and 33.1%, respectively (Fig. 4b). In comparison, N-only addition decreased the  $\text{CH}_4$  oxidation rate by 2.5% (Fig. 4a). In agreement with the field observations of  $\text{CH}_4$  uptake, concurrent additions of Fe and N, Mn and N, Cu and N enhanced the  $\text{CH}_4$  oxidation rate by 106.7%, 117.4%, and 136.5%, respectively (Fig. 4a). Adding Fe, Mn, and Cu alone increased the  $\text{CH}_4$ -oxidizing bacteria abundance by 19.9%, 32.2%, and 54.2%, respectively, while adding N decreased the  $\text{CH}_4$ -oxidizing bacteria abundance by 6.7% (Fig. 4c). At the same time, concurrent additions of Fe and N, Mn and N, or Cu and N enhanced the  $\text{CH}_4$ -oxidizing bacteria abundance by 153.7%, 165.7%, and 212.9% (Fig. 4c),

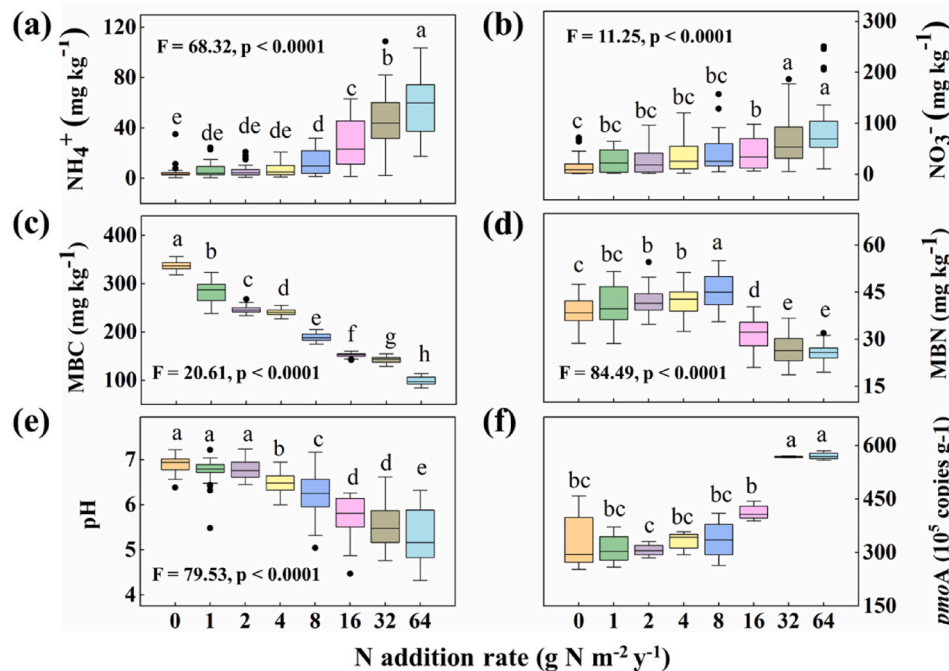


**Fig. 2.** N induced changes in other parameters in the grassland sites. N addition impacts on soil  $\text{NH}_4^+$ -N (a),  $\text{NO}_3^-$ -N (b), MBC (c), MBN (d), pH (e), *pmoA* copies (f). All data are presented as the mean  $\pm$  SE ( $n = 4$ , 1 measured for every season). Box plots show the median, first quartile, and third quartile; Different letters indicate the significance between N addition treatments at  $P = 0.05$  level.

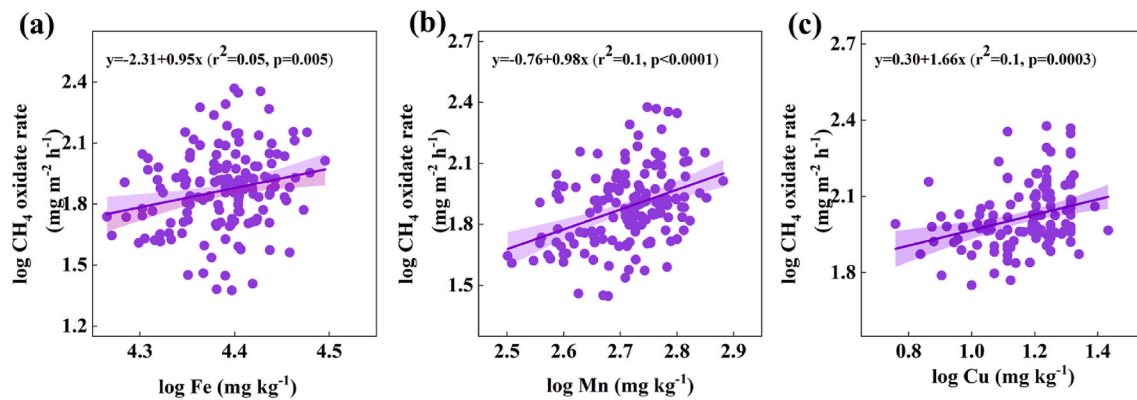


Fig. 3. The relationship between Fe (a), Mn (b), Cu (c), and  $\text{CH}_4$  uptake rate in the field experiment.

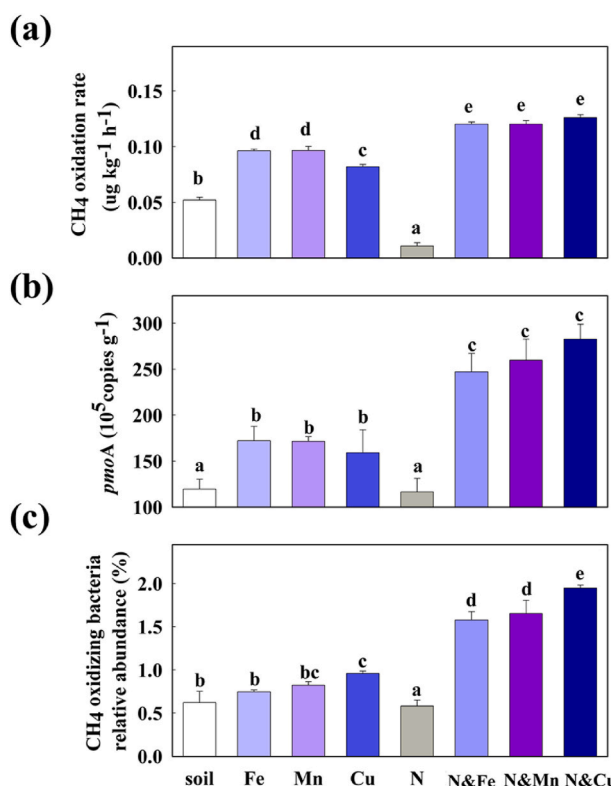


Fig. 4. The variation of  $\text{CH}_4$  oxidation rate (a), *pmoA* copies (b) and  $\text{CH}_4$  oxidizing bacteria relative abundance (c) under Fe, Mn, Cu, and N additions and their interactions in incubation. All data are presented as the mean  $\pm$  SE ( $n = 4$ ).

respectively.

### 3.3. A mechanistic understanding of $\text{CH}_4$ oxidation

A structural equation modeling (SEM) approach was applied to investigate the roles of Fe, Mn, and Cu in the microbial mechanisms of N impacts  $\text{CH}_4$  oxidation. The abundances of *pmoA* gene (Fig. 4b) and  $\text{CH}_4$ -oxidizer (Fig. 4c) were included in our models, given their established effects on  $\text{CH}_4$  oxidation and their association with N addition (Fig. 4b and c). Consistent with the observational results (Fig. 2e; Fig. S3 a), the SEMs confirmed the N-induced soil acidification. However, there was a slight difference in how soil acidification (pH decrease) affected  $\text{CH}_4$  oxidation among metal ions (Fe, Mn, and Cu) (Fig. 5a-c).

For Fe, a direct negative effect of N ( $\beta = -0.61$ ) and a positive effect

of microbe ( $\beta = 0.49$ ) on  $\text{CH}_4$  oxidation were observed (Fig. 5a). Soil acidification (pH drop) indirectly affected the  $\text{CH}_4$  oxidation by strongly suppressing soil microbial activity ( $\beta = -0.42$ ) and increasing  $\text{Fe}^{3+}$  ( $\beta = 0.1$ ). Microorganisms promoted  $\text{CH}_4$  oxidation by taking  $\text{Fe}^{3+}$  and converting them into  $\text{Fe}^{2+}$ , inferred from the negative correlation between  $\text{Fe}^{3+}$  and microorganisms. The positive correlation between microorganisms and  $\text{Fe}^{2+}$  (Fig. 5a) can be inferred from the negative correlation between  $\text{Fe}^{3+}$  and  $\text{CH}_4$  oxidation rate (Fig. S5c) and the positive correlation between  $\text{Fe}^{2+}$  and  $\text{CH}_4$  oxidation rate (Fig. S5a).

For Mn, a direct positive effect of soil microbial activity, i.e., *pmoA* abundance and  $\text{CH}_4$ -oxidizer abundance ( $\beta = 0.42$ ), and a direct negative impact of N ( $\beta = -0.61$ ) on  $\text{CH}_4$  oxidation were observed (Fig. 5b). Meanwhile, N also indirectly suppressed  $\text{CH}_4$  oxidation by strongly suppressing soil microbial activity ( $\beta = -0.84$ ) and indirectly affected soil  $\text{Mn}^{4+}$  by acidifying soil ( $\beta = -0.95$ , but the path is not significant), which positively affected  $\text{Mn}^{4+}$  ( $\beta = 0.55$ ) (Fig. 5b). Soil acidification (pH drop) indirectly affected  $\text{CH}_4$  oxidation by strongly enhancing soil microbial activity ( $\beta = 0.83$ ). Microorganisms promoted  $\text{CH}_4$  oxidation by converting  $\text{Mn}^{4+}$  to  $\text{Mn}^{2+}$ , which can be inferred from the negative correlation between  $\text{Mn}^{4+}$  and microorganisms ( $\beta = -0.86$ ), and the positive correlation between microorganisms and  $\text{Mn}^{2+}$  ( $\beta = 0.12$ ) (Fig. 5b), expressed as the negative correlation between  $\text{Mn}^{4+}$  and  $\text{CH}_4$  oxidation rate (Fig. S5d), and the positive correlation between microorganisms,  $\text{Mn}^{2+}$  and  $\text{CH}_4$  oxidation rate (Fig. S5b).

For Cu, a direct negative effect of N ( $\beta = -0.6$ ) and a positive effect of microbe ( $\beta = 0.42$ ) on  $\text{CH}_4$  oxidation were observed (Fig. 5c). Soil acidification (pH drop) indirectly affected the  $\text{CH}_4$  oxidation by increasing soil Cu content ( $\beta = 0.56$ ), which further increased  $\text{CH}_4$  oxidizers ( $\beta = 0.25$ ) and thus  $\text{CH}_4$  oxidation ( $\beta = 0.42$ ) (Fig. 5c). Taken all together, metal elements mediated the N impact on  $\text{CH}_4$  oxidation through their effects on soil microbes, but their mechanisms are different (Fig. 5a-c).

## 4. Discussion

### 4.1. Impacts of continuous high-N inputs on $\text{CH}_4$ uptake

This study quantitatively characterized the relationship between  $\text{CH}_4$  uptake and N levels (Fig. 1a; Fig. S1 a-d; Fig. S2 a-d) and found a stimulating impact on  $\text{CH}_4$  uptake under low N input while suppression impacts on  $\text{CH}_4$  uptake under high N inputs (Fig. 1b). The finding is consistent with previous studies, and it might be associated with N limitation on  $\text{CH}_4$  oxidation and competition theory (Zhang et al., 2020). A similar response of N impacts on  $\text{CH}_4$  uptake was recently reported for an alpine steppe on the Tibetan Plateau (Fig. S6) (Peng et al., 2019). These data prove that N availability strongly affects  $\text{CH}_4$  uptake, with the response magnitude depending on N addition rates. A meta-analysis reported that low N addition ( $<10 \text{ g N m}^{-2} \text{ y}^{-1}$ ) stimulated  $\text{CH}_4$  uptake

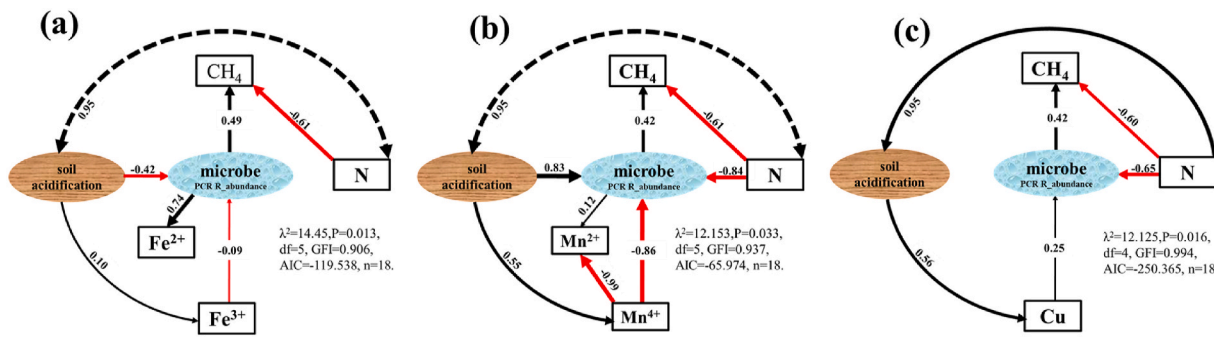


**Fig. 5.** Structural equation modeling diagrams illustrating the mechanism of soil acidification triggers trace element stimulation on  $\text{CH}_4$  oxidation. SEM of the N addition impacts on  $\text{CH}_4$  oxidation via the pathways of N addition, soil microbial activity (microbe), soil acidification (pH), and trace elements (Fe(a), Mn(b), Cu(c)). Microbe is the first principal component by soil microbial  $\text{CH}_4$ -oxidizing activity (*pmoA* abundance and  $\text{CH}_4$ -oxidizing bacteria abundance); a, Fe:  $\chi^2 = 14.45$ ,  $p = 0.013$ ,  $df = 5$ , Goodness of Fit Index (GFI) = 0.91, Akaike Information Criterion (AIC) = -119.54, and  $n = 18$ ; b, Mn:  $\chi^2 = 12.15$ ,  $p = 0.033$ ,  $df = 5$ , Goodness of Fit Index (GFI) = 0.94, Akaike Information Criterion (AIC) = -65.97, and  $n = 18$ ; c, Cu:  $\chi^2 = 12.13$ ,  $p = 0.016$ ,  $df = 4$ , Goodness of Fit Index (GFI) = 0.99, Akaike Information Criterion (AIC) = -250.37, and  $n = 18$ ; Red and black solid arrows represent significant negative and positive effects ( $p < 0.05$ ), respectively, dotted lines represent the insignificant paths. Values associated with the arrows represent standardized path coefficients.

(Aronson and Helliker, 2010), while high N addition ( $>10 \text{ g N m}^{-2} \text{ y}^{-1}$ ) inhibited  $\text{CH}_4$  uptake. In another study (Geng et al., 2017),  $\text{CH}_4$  uptake peaked at a lower N addition rate ( $1 \text{ g N m}^{-2} \text{ year}^{-1}$ ), which was explained by N limitation. Under N-limited conditions, N application was found to either relieve the N limitation of methanotrophic community or stimulate the biosynthesis of the enzymes involved in  $\text{CH}_4$  oxidation (King, 1992). The reported declining trend in  $\text{CH}_4$  uptake may have occurred due to the competition between  $\text{NH}_4^+$  and  $\text{CH}_4$  (Dunfield and Knowles, 1995; Schimel and Guldledge, 1998) or N's toxic impact on methanotrophs (Dunfield and Knowles, 1995). Soil  $\text{NH}_4^+$  concentration is directly associated with soil  $\text{CH}_4$  oxidation rate. The  $\text{NH}_4^+$  molecule

inhibits  $\text{CH}_4$  oxidation by competing for the binding site of the  $\text{CH}_4$  mono-oxygenase enzyme (Bodelier and Laanbroek, 2004). In the present study, a negative relationship between inorganic N and  $\text{CH}_4$  uptake (Fig. 6f) was found. The suppressed  $\text{CH}_4$  uptake may be attributed to the inhibitory effects of hydroxylamine and nitrite inhibitory, two intermediate products of nitrification (Bodelier and Laanbroek, 2004). The nonlinear response pattern of soil bacterial diversity (including Chao1, observed\_species, pD\_whole\_tree, and Shannon diversity index) might be relevant to the reported unimodal response to N addition by methanotrophic bacteria (Fig. S7). Further investigations to examine the mechanisms of microbial regulation of  $\text{CH}_4$  oxidation are deemed critical for

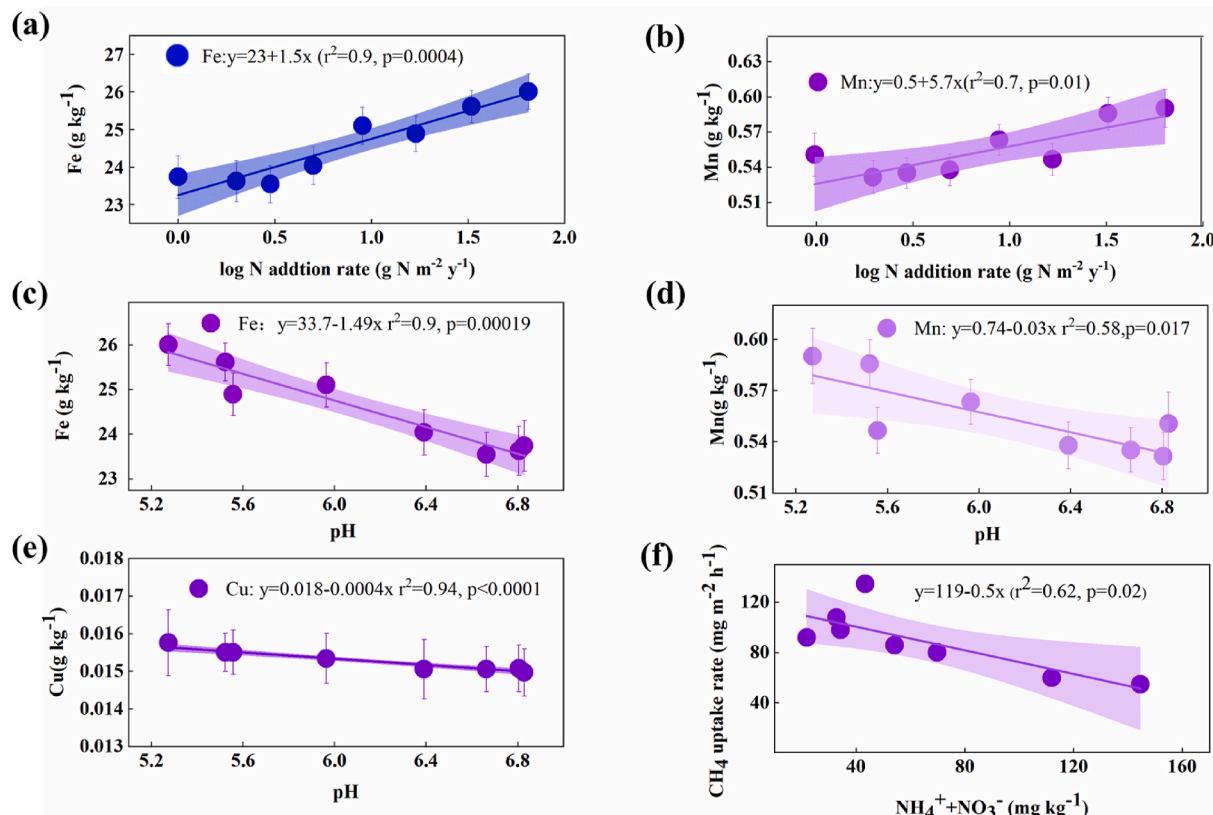


**Fig. 6.** The increase in soil Fe (a) and Mn (b) content with nitrogen application rate in a field experiment. The relationship between Fe (c), Mn (d), Cu (e), and pH across control and all nitrogen addition treatments. The relationship between  $\text{NH}_4^+ + \text{NO}_3^-$  and  $\text{CH}_4$  uptake rate to N addition across control and all nitrogen addition treatments (f).

understanding the N impacts on  $\text{CH}_4$  cycling.

#### 4.2. Soil acidification triggered the trace element's stimulation on $\text{CH}_4$ oxidation

Based on our experimental results and theoretical framework, we speculated three mechanisms to explain the N-induced acidification triggered the stimulation of  $\text{CH}_4$  oxidation. First, long-term N addition acidified soils, leading to soil  $\text{pH} < 5.7$  which corresponded to the threshold of N impacts on  $\text{CH}_4$  (Fig. 2e; Fig. S3 a). Under  $\text{pH} < 5.7$ , soil metal ions were desorbed from soils particles, leading to an accumulation of soil Fe, Mn (Fig. 6a and b; Fig. S5), which was in agreement with studies in the same site (Tian et al., 2016), and other regions (Ernani et al., 2002; Raza et al., 2020). Soil pH is a critical factor controlling  $\text{CH}_4$  oxidation (Saarnio et al., 2004) and was positively correlated with the  $\text{CH}_4$  uptake along N application (Fig. S3 b). In our study, the positive relationship between  $\text{Fe}^{2+}$  and  $\text{Mn}^{2+}$  with  $\text{CH}_4$  oxidation rate in the incubation experiment (Figs. S5a and b), the negative relationship between Fe and Mn element with pH (soil acidification stimulated elemental release from soil minerals) in the field experiment were reported (Fig. 6c and d).

Second, increased N addition promoted the abundance of  $\text{CH}_4$  oxidation gene *pmoA* (Fig. 2f). N also shifted bacterial communities (Fig. S7) toward more putatively copiotrophic bacterial taxa (Liu et al., 2020). This community shift may have contributed to the increased enzymes that can oxidize  $\text{CH}_4$  with Fe (III) and Mn (IV) minerals as electron acceptors (Oni and Friedrich, 2019). Therefore, we conjectured that an unknown methanotrophic bacteria might have participated in the  $\text{CH}_4$  oxidization with Fe (III) and Mn (IV) minerals as electron acceptors (Oni and Friedrich, 2019). The inconsistent effects of N application on  $\text{CH}_4$  uptake and *pmoA* in the experiment (Fig. 1a; Fig. 2f) are noteworthy and can be explained by the competition between  $\text{NH}_4^+$  and  $\text{CH}_4$  for *pmoA* (Schimel and Guldge, 1998). Due to the microbial N transformations with N additions, both  $\text{NH}_4^+$  and  $\text{NO}_3^-$  contents increased (Fig. 2a and b). As external  $\text{NH}_4^+$  entered the soils (Fig. 2a), methanotrophic bacteria converted ammonia to nitrite, consuming oxygen ( $\text{O}_2$ ) and leading to an anaerobic microenvironment (Fig. 7), thus leading to  $\text{CH}_4$  oxidization with Fe (III) and Mn (IV) minerals as electron acceptors (Fig. 7). And this can be confirmed by our incubation experiments, in which the positive relationship between  $\text{Fe}^{2+}$ ,  $\text{Mn}^{2+}$ , and  $\text{CH}_4$  oxidation rate, and the negative relationship between  $\text{Fe}^{3+}$ ,  $\text{Mn}^{4+}$ , and  $\text{CH}_4$  oxidation rate were observed (Fig. S5).

A third potential mechanism is the positive impact of Cu on  $\text{CH}_4$  monooxygenase (MMO) (Hakeman and Rosenzweig, 2007; Stein, 2020). This is built upon the positive correlation between concentrations of the *pmoA* transcript and the Cu levels (Choi et al., 2003), as confirmed in this study by the positive correlation between Cu content and  $\text{CH}_4$  uptake rate (Fig. 3c) and negative correlation between pH and Cu content (Fig. 6e). Soil acidification enhanced the activity of copper-containing enzymes or compounds (such as methanobactin) produced by methanotrophs (Chang et al., 2018). The production and release of reactive intermediates (related enzymes or compounds) by microorganisms can be strongly enhanced by copper availability, further altering the rate of  $\text{CH}_4$  oxidation by activating copper-containing enzymes (Beal et al., 2009; Ettwig et al., 2016).

#### 4.3. A conceptual model for trace-elements mediation of $\text{CH}_4$ oxidation

We proposed a conceptual framework to summarize the previous mechanisms to explain the relieved suppression of  $\text{CH}_4$  oxidation under cumulative-high N addition (Fig. 7). After long-term N addition,  $\text{H}^+$  accumulated and pH declined (Schroder et al., 2011; Tian et al., 2016; Xiao et al., 2020) (Fig. 2e). With declining soil pH, exchangeable soil cations such as Fe, Mn, and Cu desorbed from the cation exchange sites (Schroder et al., 2011; Rezapour, 2014; Zhang et al., 2017; Yang et al., 2018) (Fig. 7; Fig. 5a-c; Fig. S4). Soil acidification has been found to enhance the availability of metal elements ( $\beta = 0.1$  for  $\text{Fe}^{3+}$ ,  $\beta = 0.55$  for  $\text{Mn}^{4+}$ ,  $\beta = 0.56$  for Cu) (Fig. 5a-c; Fig. 6 c-e). Moreover, the *pmoA* gene (Fig. 2f; Fig. S3 c), the concentrations of soil  $\text{NH}_4^+$  (Fig. 2a) and  $\text{NO}_3^-$  (Fig. 2b) were observed significantly increase with the N application rate while  $\text{CH}_4$  uptake (Fig. 1a) first increased then decreased with the N application rate. And Fe, Mn, and Cu have stimulated impaction on the  $\text{CH}_4$  oxidation (Fig. 4a), the abundances of *pmoA* gene (Fig. 4b) and  $\text{CH}_4$ -oxidizers (Fig. 4c). Based on the above results and previous studies (Ettwig et al., 2010; Xiao et al., 2020), the hypothesis that higher available metal elements stimulate  $\text{CH}_4$  oxidation was supported as indicated by the *pmoA* expression (Fig. 7). The rapid  $\text{O}_2$  consumption by other microbes may have created anoxic microenvironments and provided abundant substrates for acetoclastic methanogenesis (Angle et al., 2017). Therefore, metal elements, such as Fe, Mn are electron acceptors substituting oxygen to complete the  $\text{CH}_4$  oxidation process (Stein, 2020).

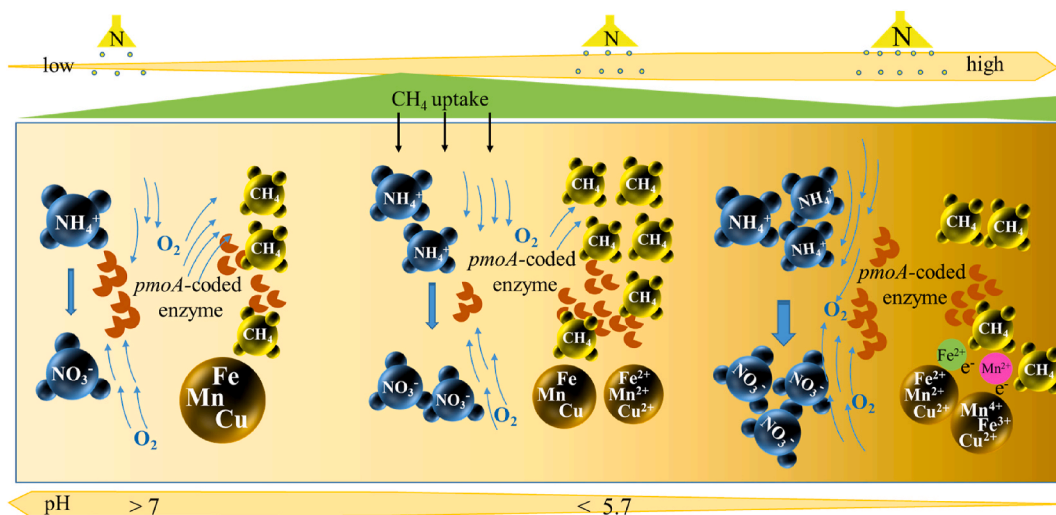


**Fig. 7.** Conceptual diagram illustrating the mechanisms of soil acidification triggered trace element mediating on  $\text{CH}_4$  oxidation along high N accumulation. Long-term N addition induced soil acidification, stimulating the release of soil ions from soil particles. The oxidation of elevated  $\text{NH}_4^+$  to  $\text{NO}_3^-$  consumed much oxygen. Then, activated trace elements due to soil acidification could be used as an alternative electron acceptor for the  $\text{CH}_4$  oxidation during long-term N enrichment.

#### 4.4. Limitations and future work

Although the substantial impact of N addition on  $\text{CH}_4$  oxidation has been well established (Stein, 2020), this study reported a novel finding on the N impact on  $\text{CH}_4$  oxidation through changing metal element availabilities. Two major limitations have been identified and must be addressed in future work. First, no experimental studies have been conducted to characterize soil metal elements along an N addition gradient over the long term and focused on how eventual concentration changes affect  $\text{CH}_4$  oxidation across N limitation to saturation scenarios (Peng et al., 2019). The question remains whether there is a general cognition on the relationship between  $\text{CH}_4$  oxidation and soil metal element along the N addition gradient (Hakeman and Rosenzweig, 2007) in semiarid grassland ecosystems. The significant impacts of Fe, Mn, and Cu on  $\text{CH}_4$  oxidation, *pmoA*, and  $\text{CH}_4$ -oxidizing bacteria abundance (Fig. 4a–c) and the correlation between Fe, Mn, and  $\text{CH}_4$  oxidation rate (Fig. S5) in our incubation experiment confirmed our conceptual framework and offering reliable foundation.

Second, we used the functional gene abundance to represent the  $\text{CH}_4$  oxidation potential and its association with the  $\text{CH}_4$  oxidation rate at the ecosystem level. We focused on the total  $\text{CH}_4$ -oxidizer community and used the abundances of *pmoA* and  $\text{CH}_4$ -oxidizer as indicators for soil microbial activity (PC); the specific genes related to the enzymes for Fe, Mn, and Cu association with  $\text{CH}_4$  oxidation were not measured in the present study and will be investigated in the future.

#### 5. Conclusion

This study established an ecosystem-scale mechanistic link between N-led soil acidification and  $\text{CH}_4$  uptake transition under long-term N addition, implying the vital role of metal elements on  $\text{CH}_4$  oxidation during soil acidification. The pH value of 5.7 during soil acidification represents a critical threshold of metal elements affecting  $\text{CH}_4$  cycling in soils. We thus highlighted the importance of metal elements in mediating  $\text{CH}_4$  oxidation under future elevated N deposition, which is critical for understanding the  $\text{CH}_4$  cycle under future N deposition.

To the best of our knowledge, this study represented the first attempt to report the metal element-mediated  $\text{CH}_4$  oxidation in the aerobic environment of a semi-arid grassland. Consequently, the novel findings of continuous high N-input in alleviating N suppression of  $\text{CH}_4$  oxidation contribute to better predictability of the  $\text{CH}_4$  cycle under changing environments, particularly considering the projected climbing atmospheric N depositions. The metal impact on  $\text{CH}_4$  oxidation has yet to be incorporated into process-based  $\text{CH}_4$  models (Xu et al., 2016); this study provides mechanistic knowledge to fill this gap.

#### Declaration of competing interest

The authors declare that they have no known competing financial interests or personal relationships that could have appeared to influence the work reported in this paper.

#### Data availability

Data will be made available on request.

#### Acknowledgments

This study was partially supported by the National Natural Science Foundation of China (32271681, 41125001, 4137111, 32171873) and the Joint Funds of China's National Natural Science Foundation (U2006215), and by Key Laboratory of Ecology and Environment in Minority Areas (Minzu University of China), National Ethnic Affairs Commission (KLEEMA202206). X.X. acknowledged the financial assistance provided by the National Science Foundation (2145130) and SPRUCE and NGE Arctic projects, supported by the Office of Biological

and Environmental Research in the Department of Energy Office of Science. I.A.J. acknowledges support from the European Research Council Synergy Grant IMBALANCE-P (ERC-2013-SyG-610028).

#### Appendix A. Supplementary data

Supplementary data to this article can be found online at <https://doi.org/10.1016/j.soilbio.2023.109098>.

#### References

Ambus, P., Robertson, G.P., 2006. The effect of increased N deposition on nitrous oxide, methane and carbon dioxide fluxes from unmanaged forest and grassland communities in Michigan. *Biogeochemistry* 79, 315–337.

Amos, R.T., Bekins, B.A., Cozzarelli, I.M., Voytek, M.A., Kirshtein, J.D., Jones, E.J., Blows, D.W., 2012. Evidence for iron-mediated anaerobic methane oxidation in a crude oil-contaminated aquifer. *Geobiology* 10, 506–517.

Angle, J.C., Morin, T.H., Soden, L.M., Narro, A.B., Smith, G.J., Borton, M.A., Rey-Sanchez, C., Daly, R.A., Mirfenderesgi, G., Hoyt, D.W., Riley, W.J., Miller, C.S., Bohrer, G., Wrighton, K.C., 2017. Methanogenesis in oxygenated soils is a substantial fraction of wetland methane emissions. *Nature Communications* 8, 1567.

Arnoni, E.L., Helliker, B.R., 2010. Methane flux in non-wetland soils in response to nitrogen addition: a meta-analysis. *Ecology* 91, 3242–3251.

Beal, E.J., House, C.H., Orphan, V.J., 2009. Manganese- and iron-dependent marine methane oxidation. *Science* 325, 184–187.

Bodelier, P.L.E., Roslev, P., Henckel, T., Frenzel, P., 2000. Stimulation by ammonium-based fertilizers of methane oxidation in soil around rice roots. *Nature* 403, 421–424.

Bodelier, P.L.E., Laanbroek, H.J., 2004. Nitrogen as a regulatory factor of methane oxidation in soils and sediments. *FEMS Microbiology Ecology* 47, 265–277.

Boiesen, A., Arvin, E., Broholm, K., 1993. Effect of mineral nutrients on the kinetics of methane utilization by methanotrophs. *Biodegradation* 4, 163–170.

Breemen, N.V., Burrough, P.A., Velthorst, E.J., van Dobben, H.F., Wit, T., Ridder, T.D., Reijnders, H.F.R., 1982. Soil acidification from atmospheric ammonium sulphate in forest canopy throughfall. *Nature* 299, 548–550.

Cai, Y., Zheng, Y., Bodelier, P.L., Conrad, R., Jia, Z., 2016. Conventional methanotrophs are responsible for atmospheric methane oxidation in paddy soils. *Nature Communications* 7, 11728.

Chang, J., Gu, W., Park, D., Semrau, J.D., DiSpirito, A.A., Yoon, S., 2018. Methanobactin from *Methylosinus trichosporium* OB3b inhibits N<sub>2</sub>O reduction in denitrifiers. *The ISME Journal* 12, 2086–2089.

Choi, D.W., Kunz, R.C., Boyd, E.S., Semrau, J.D., Antholite, W.E., Han, J.I., Zahn, J.A., Boyd, J.M., de la Mora, A.M., DiSpirito, A.A., 2003. The membrane-associated methane monooxygenase (pMMO) and pMMO-NADH:quinone oxidoreductase complex from *Methylococcus capsulatus* Bath. *Journal of Bacteriology* 185, 5755–5764.

Dalal, R.C., Allen, D.E., Livesley, S.J., Richards, G., 2008. Magnitude and biophysical regulators of methane emission and consumption in the Australian agricultural, forest, and submerged landscapes: a review. *Plant and Soil* 309, 43–76.

Dijkstra, F.A., Morgan, J.A., Follett, R.F., Lecain, D.R., 2013. Climate change reduces the net sink of  $\text{CH}_4$  and  $\text{N}_2\text{O}$  in a semiarid grassland. *Global Change Biology* 19, 1816–1826.

DiSpirito, A.A., Semrau, J.D., Murrell, J.C., Gallagher, W.H., Dennison, C., Vuilleumier, S., 2016. Methanobactin and the link between copper and bacterial methane oxidation. *Microbiology and Molecular Biology Reviews* 80, 387–409.

Dunfield, P., Knowles, R., 1995. Kinetics of inhibition of methane oxidation by nitrate, nitrite, and ammonium in a humisol. *Applied Aan Environmental Microbiology* 61, 3129–3135.

Ernani, P.R., Bayer, C., Maestri, L., 2002. Corn yield as affected by liming and tillage System on an acid Brazilian oxisol. *Agronomy Journal* 94, 305–309.

Ettwig, K.F., Butler, M.K., Le Paslier, D., Pelletier, E., Mangenot, S., Kuyper, M.M., Schreiber, F., Dutilh, B.E., Zedelius, J., de Beer, D., Goerich, J., Wessels, H.J., van Aken, T., Luesken, F., Wu, M.L., van de Pas-Schoonen, K.T., Op den Camp, H.J., Janssen-Megens, E.M., Francoijis, K.J., Stunnenberg, H., Weissenbach, J., Jetten, M.S., Strous, M., 2010. Nitrite-driven anaerobic methane oxidation by oxygenic bacteria. *Nature* 464, 543–548.

Ettwig, K.F., Zhu, B., Speth, D., Keltjens, J.T., Jetten, M.S.M., Kartal, B., 2016. Archaea catalyze iron-dependent anaerobic oxidation of methane. *Proceedings of the National Academy of Sciences* 113, 12792–12796.

Ferri, R., Donna, F., Smith, D.R., Guazzetti, S., Zacco, A., Rizzo, L., Bontempi, E., Zimmerman, N.J., Lucchini, R.G., 2012. Heavy metals in soil and salad in the proximity of historical ferroalloy emission. *Journal of Environmental Protection* 3, 374–385.

Geng, J., Cheng, S., Fang, H., Yu, G., Li, X., Si, G., He, S., Yu, G., 2017. Soil nitrate accumulation explains the nonlinear responses of soil  $\text{CO}_2$  and  $\text{CH}_4$  fluxes to nitrogen addition in a temperate needle-broadleaved mixed forest. *Ecological Indicators* 79, 28–36.

Gulledge, J., Hrywna, Y., Cavanaugh, C., Steudler, P.A., 2004. Effects of long-term nitrogen fertilization on the uptake kinetics of atmospheric methane in temperate forest soils. *FEMS Microbiology Ecology* 49, 389–400.

Hakeman, A.S., Rosenzweig, A.C., 2007. The biochemistry of methane oxidation. *Annual Review of Biochemistry* 76, 223–241.

Horswill, A.R., Nauseef, W.M., 2008. Host interception of bacterial communication signals. *Cell Host & Microbe* 4, 507–509.

Hütsch, B.W., 2001. Methane oxidation in arable soil as inhibited by ammonium, nitrite, and organic manure with respect to soil pH. *Biology and Fertility of Soils* 28, 27–35.

King, G.M., 1992. Ecological aspects of methane oxidation, a key determinant of global methane dynamics. *Advances in Microbial Ecology* 12, 431–468.

Krause, S.M., Johnson, T., Samadhi Karunaratne, Y., Fu, Y., Beck, D.A., Chistoserdova, L., Lidstrom, M.E., 2017. Lanthanide-dependent cross-feeding of methane-derived carbon is linked by microbial community interactions. *Proceedings of the National Academy of Sciences* 114, 358–363.

Lindsay, W.L., Norvell, W.A., 1978. Development of a DTPA soil test for zinc, iron, manganese, and copper. *Soil Science Society of America Journal* 3, 421–428.

Liu, W., Jiang, L., Hu, S., Li, L., Liu, L., Wan, S., 2014. Decoupling of soil microbes and plants with increasing anthropogenic nitrogen inputs in a temperate steppe. *Soil Biology and Biochemistry* 72, 116–122.

Liu, W., Jiang, L., Yang, S., Wang, Z., Tian, R., Peng, Z., Chen, Y., Zhang, X., Kuang, J., Ling, N., Wang, S., Liu, L., 2020. Critical transition of soil bacterial diversity and composition triggered by nitrogen enrichment. *Ecology* 8, e03053.

Livesley, S.J., Kiese, R., Michle, P., Weston, C.J., Butterbach-Bahl, K., Arndt, S.K., 2009. Soil-atmosphere exchange of greenhouse gases in a *Eucalyptus marginata* woodland, a clover-grass pasture, and *Pinus radiata* and *Eucalyptus globulus* plantations. *Global Change Biology* 15, 425–440.

Malik, A.A., Puissant, J., Buckeridge, K.M., Goodall, T., Jehmlich, N., Chowdhury, S., Gweon, H.S., Peyton, J.M., Mason, K.E., van Agtmaal, M., Blaud, A., Clark, I.M., Whitaker, J., Pywell, R.F., Ostle, N., Gleixner, G., Griffiths, R.I., 2018. Land use driven change in soil pH affects microbial carbon cycling processes. *Nature Communications* 9, 3591.

Oni, O.E., Friedrich, M.W., 2019. Metal oxide reduction linked to anaerobic methane oxidation. *Trends in Microbiology* 25, 88–90.

Peng, Y., Wang, G., Li, F., Yang, G., Fang, K., Liu, L., Qin, S., Zhang, D., Zhou, G., Fang, H., Liu, X., Liu, C., Yang, Y., 2019. Unimodal response of soil methane consumption to increasing nitrogen additions. *Environmental Science and Technology* 53, 4150–4160.

Raza, S., Miao, N., Wang, P., Ju, X., Chen, Z., Zhou, J., Kuzyakov, Y., 2020. Dramatic loss of inorganic carbon by nitrogen-induced soil acidification in Chinese croplands. *Global Change Biology* 26, 3738–3751.

Reischer, G.H., Ebdon, J.E., Bauer, J.M., Schuster, N., Ahmed, W., Astrom, J., Blanch, A. R., Bloschl, G., Byamukama, D., Coakley, T., Ferguson, C., Goshu, G., Ko, G., de Roda Husman, A.M., Mushi, D., Poma, R., Pradhan, B., Rajal, V., Schade, M.A., Sommer, R., Taylor, H., Toth, E.M., Vrajmasu, V., Wuertz, S., Mach, R.L., Farnleitner, A.H., 2013. Performance characteristics of qPCR assays targeting human- and ruminant-associated bacteroidetes for microbial source tracking across sixteen countries on six continents. *Environmental Science and Technology* 47, 8548–8556.

Rezapour, S., 2014. Effect of sulfur and composted manure on  $\text{SO}_4^{2-}$ , P and micronutrient availability in a calcareous saline-sodic soil. *Chemistry and Ecology* 30, 147–155.

Saarnio, L., Wittenmayer, S., Merbach, W., 2004. Rhizospheric exudation of *Eriophorum vaginatum* L. – potential link to methanogenesis. *Plant and Soil* 267, 343–355.

Schimel, J.P., Guldge, J., 1998. Microbial community structure and global trace gases. *Global Change Biology* 7, 745–758.

Schroder, J.L., Zhang, H.L., Girma, K., Raun, W.R., Penn, C.J., Payton, M.E., 2011. Soil acidification from long-term use of nitrogen fertilizers on winter wheat. *Soil Fertility & Plant Nutrition* 75, 957–964.

Semrau, J.D., DiSpirito, A.A., Yoon, S., 2010. Methanotrophs and copper. *Microbiology Reviews* 34, 496–531.

Semrau, J.D., Jagadevan, S., DiSpirito, A.A., Khalifa, A., Scanlan, J., Bergman, B.H., Freemeier, B.C., Baral, B.S., Bandow, N.L., Vorobev, A., Haft, D.H., Vuilleumier, S., Murrell, J.C., 2013. Methanobactin and MmoD work in concert to act as the ‘copper-switch’ in methanotrophs. *Environmental Microbiology* 15 (11), 3077–3086.

Stein, L.Y., 2020. The long-term relationship between microbial metabolism and greenhouse gases. *Trends in Microbiology* 28, 500–511.

Tian, Q., Liu, N., Bai, W., Li, L., Chen, J., Reich, P.B., Yu, Q., Guo, D., Smith, M.D., Knapp, A.K., Cheng, W., Lu, P., Gao, Y., Yang, A., Wang, T., Li, X., Wang, Z., Ma, Y., Han, X., Zhang, W.H., 2016. A novel soil manganese mechanism drives plant species loss with increased nitrogen deposition in a temperate steppe. *Ecology* 97, 65–74.

Thustos, P., Willison, T.W., Baker, J.C., Murph, D.V., Pavlikova, D., Goulding, K.W.T., Powson, D.S., 1998. Short-term effects of nitrogen on methane oxidation in soils. *Soil Biology and Fertility of Soils* 28, 64–70.

Visvanathan, C., Pokhrel, D., Cheimchaisri, W., Hettiaratchi, J.P.A., Wu, J.S., 1999. Methanotrophic activities in tropical landfill cover soils: effects of temperature, moisture content and methane concentration. *Waste Management & Research* 17 (4), 313–323.

Wang, Y., Hu, X., 2016. *Inorganic and Analytical Chemistry*, fourth ed. Science Press, Bei Jing.

Xiao, H., Wang, B., Lu, S., Chen, D., Wu, Y., Zhu, Y., Hu, S., Bai, Y., 2020. Soil acidification reduces the effects of short-term nutrient enrichment on plant and soil biota and their interactions in grasslands. *Global Change Biology* 26, 4626–4637.

Xu, X., Yuan, F., Hanson, P.J., Wullschleger, S.D., Thornton, P.E., Riley, W.J., Song, X., Graham, D.E., Song, C., Tian, H., 2016. Review and Synthesis: four decades of modeling methane cycling within terrestrial ecosystems. *Biogeosciences* 13, 3735–3755.

Yang, X., Shao, M.a., Li, T., 2020. Effects of terrestrial isopods on soil nutrients during litter decomposition. *Geoderma* 376, 11454.

Yang, X.D., Ni, K., Shi, Y.Z., Yi, X.Y., Zhang, Q.F., Fang, L., Ma, L.F., Ruan, J.Y., 2018. Effects of long-term nitrogen application on soil acidification and solution chemistry of a tea plantation in China. *Agriculture, Ecosystems & Environment* 252, 74–82.

Zhang, L., Guo, D., Niu, S., Wang, C., Shao, C., Li, L., 2012. Effects of mowing on methane uptake in a semiarid grassland in northern China. *PLoS One* 7, e35952.

Zhang, L., Yuan, F., Bai, J., Duan, H., Gu, X., Hou, L., Huang, Y., Yang, M., He, J.S., Zhang, Z., Yu, L., Song, C., Lipson, D.A., Zona, D., Oeche, W., Janssens, I.A., Xu, X., 2020. Phosphorus alleviation of nitrogen-suppressed methane sink in global grasslands. *Ecology Letters* 23, 821–830.

Zhang, L.H., Huo, Y.W., Guo, D.F., Wang, Q.B., Bao, Y., Li, L.H., 2014. Effects of multi-nutrient additions on GHG fluxes in a temperate grassland of northern China. *Ecosystems* 17, 657–672.

Zhang, Y.T., de Vries, W., Thomas, B.W., Hao, X.Y., Shi, X.J., 2017. Impacts of long-term nitrogen fertilization on acid buffering rates and mechanisms of a slightly calcareous clay soil. *Geoderma* 305, 92–99.